# Temporal-spatial pattern and driving factors of cultivated land use transition at country level in Shaanxi province, China

**Zhe Chen · Xiaojing Li · Xianli Xia**

**Abstract** The county-level Cultivated Land Use Form index (CLUF) in Shaanxi province in 2000, 2005, 2010, and 2015 was measured with the entropy method and the linear combination method. Then, the spatial differentiation characteristics and driving mechanism of CLUF were characterized and identified through exploratory spatial data analysis, standard deviation ellipse model, kernel density estimation, multiple linear, and spatial regression analysis. The conclusions drawn from empirical results were as follows. First, the CLUF presented a spatial differentiation pattern of high in the middle and low in the north and south, and the CLUF had a strong positive spatial correlation. The local spatial patterns were mainly the high-high agglomeration and low-low agglomeration. Second, the gravity center of CLUF moves from northeast to southwest, but it is always located in the central part of Shaanxi province. The CLUF showed a trend from expansion and decentralization to contraction and centralization in geographical space, with an obvious spatial spillover effect. Third, the results of nuclear density estimation showed that the difference in the CLUF between counties displayed a trend of first shrinking and then expanding. Fourth, the cultivated land use transition was promoted by the combination of the natural environment, economic growth, and urbanization development, and factors of the driving mechanism of the cultivated land use transition are complicated. Finally, policy recommendations to promote the rationalization and cultivated land use transition were put forward, such as strengthening infrastructure construction, formulating differentiated policies, and giving play to the role of neighboring demonstrations.

**Keywords** Cultivated land use · Transition · Spatial distribution · Driving mechanism · Land use

Zhe Chen and Xiaojing Li are co-first authors of the article.

Z. Chen · X. Xia (✉)
School of Economics and Management, Northwest Agriculture and Forestry University, Yangling, China
e-mail: xnxxli@nwafu.edu.cn

Z. Chen
e-mail: xncz@nwafu.edu.cn

X. Li
School of Economics and Management, Yan Tai University, Yantai, China
e-mail: xnlxj@nwafu.edu.cn

## Introduction

The land is the space carrier of human social and economic activities, the most fundamental material basis for production, and an essential part of global sustainable development (Perring et al., 2013). The importance and scarcity of land resources highlight the significance of following the objective laws of land use and the primary goals of optimizing land use structure and improving land use efficiency

(Duro et al., 2020; Liu et al., 2020a, b). Land use transition refers to the temporal and spatial changes in regional land use patterns in a specific period driven by social and economic changes and innovations, with noticeable changes in both quantity and structure and hidden changes in quality and property rights. It is the process of changing land types from one form to another until achieving the coordinated development of land use, social economy, and ecological environment (Long et al., 2019). Land use transition research refers to the study of the process and trend of land use transition with scientific research methods to reveal and characterize the evolutionary law of land use transition and adjust the objective contradictions between different land use forms. This research is expected to alleviating the tension in the "man-earth relationship" and realizing innovative land resource management (Liu et al., 2020a, b). Therefore, research on the spatial evolution process and driving factors of regional land use transition in the context of urbanization and industrialization is of practical significance for realizing regional sustainable development.

Cultivated land and woodland are the most productive land types. The former is the core element of land resource because it bears the responsibilities of food production and material supply, which is an important guarantee of national food security and ecological security. Therefore, cultivated land use transition has always been the focus of land use transition research. However, the land use transition research began with woodland transition research. Mather and Needle (1998) investigated the trend of forest area in different countries and put forward forest transition theory (Mather & Needle, 1998). Then, scholars began to explore the causes, connotations and concepts, transition models, and influencing factors of land use transition, which greatly enriched the content of land use transition research (Brian & Daniel, 2004; Zeilhofer et al., 2014). Meanwhile, scholars have gradually expanded their research perspectives and have conducted in-depth research from the perspective of transition concepts, methods, and influencing factors. For example, Ge et al. (2018) constructed a theoretical model of cultivated land use transition using per capita cultivated land area indicators, which explored the coupling relationship and the internal mechanism between cultivated land use transition and food production in China (Ge et al., 2018). Song and Li

(2019) constructed a comprehensive explanatory framework for the available cultivated land use transition and studied the internal relationship between induced production substitution and the evolution of cultivated land use type structure, input structure, and planting structure with quantitative methods (Song & Li, 2019). Xiang et al. (2016) measured the status of cultivated land use transition from spatial form and functional form, analyzed the spatial characteristics of cultivated land use transition adopting the spatial autocorrelation model, and delved into the influencing factors of spatial differentiation of cultivated land use transition from the aspects of population, economy, and industrial structure applying the radial basis function neural network model (Wang & Zhang, 2021). Most of the existing researches focused on the process, mode, and mechanism of cultivated land use transition from the perspectives of cultivated land quantity and spatial function. However, in recent years, driven by social and economic changes and innovation, cultivated land use transition has gone far beyond the scope of its quantity and structure, and it is a continuous evolution of cultivated land use patterns (Long et al., 2019). Therefore, the study on cultivated land use transition from the change process of CLUF is of significance.

In recent years, the accelerating urbanization in China has caused an extreme shortage of urban construction land. Meanwhile, the migration of the youth from the rural areas to developed urban areas has also resulted in the abandonment of large areas of rural arable land and the deterioration of the utilization quality, which seriously hinders the arable land use efficiency (Wang et al., 2020a, b, c). Simultaneously, the shortage of urban construction land has intensified the contradiction between land supply and demand. The urban encroachment on cultivated land in the outskirts of cities has intensified the damage to cultivated land resources (Tang et al., 2020). All issues mentioned have given the urgency of the balance of cultivated land quantity, prevention of the degradation of cultivated land quality, improvement of the cultivated land use efficiency, and the promotion of the national cultivated land use transition (Deng, 2020). Therefore, the primary purpose of this research is to construct a scientific and reasonable conceptual framework for cultivated land use transition, to explore the temporal and spatial

differentiation pattern of cultivated land use transition and its driving mechanism, and to provide a reference for the efficient use of cultivated land and regional sustainable development.

## Study area

Located in the northwest region of China, Shaanxi province is mainly composed of 107 counties under the jurisdiction of 10 prefecture-level cities, covering an administrative area of 205,600 square kilometers (Fig. 1). The terrain of Shaanxi province is high in the north and south regions and low in the middle regions, mainly composed of northern Shaanxi loess plateau, central Guan Zhong plain, and southern Shaanxi mountainous area. By the end of 2018, the total land area of Shaanxi province was 20,562,400 hectares, of which the area of cultivated land was only 3,976,800 hectares, accounting for 19.34%. With the rapid development of urbanization, the urban construction land in Shaanxi province is in increasing demand, and consequent encroachment on arable land resources has resulted in a slump in the quantity and quality of cultivated land. The land use type and cultivated land use mode in this region are experiencing rapid transformation.

## Methodology and data

### Measurement of CLUF index

The Cultivated Land Use Form (CLUF) is the core content of land use transformation that is the product of land use change evolution to a particular stage and period (Ma et al., 2020). Some scholars have pointed out two forms of the CLUF: dominant form and recessive form. The former is presented by land use quantity, structure, and spatial pattern, while the latter is presented by quality, property right, management mode, input, output, and function (Chen et al., 2014; Long & Qu, 2018). In recent years, the implementation of China's urbanization and rural revitalization strategy has promoted the remarkable transition of rural cultivated land (Fig. 2), which was reflected in two aspects: Land Use Dominant Form (CLDF), and Land Use Recessive Form (CLRF). The CLDF mainly covers the quantity, structure, and spatial pattern of cultivated land use, while the CLRF is reflected by quality, property right, mode of operation, inherent input, and output capacity (Ge et al., 2018).

In this study, the CLUF was presented by the CLDF and CLRF (Table 1). For the CLDF, the per-capita cultivated land area (PCLA) and per-capita grain sown area (PGSA) were firstly selected to represent the quantity of cultivated land use. The most
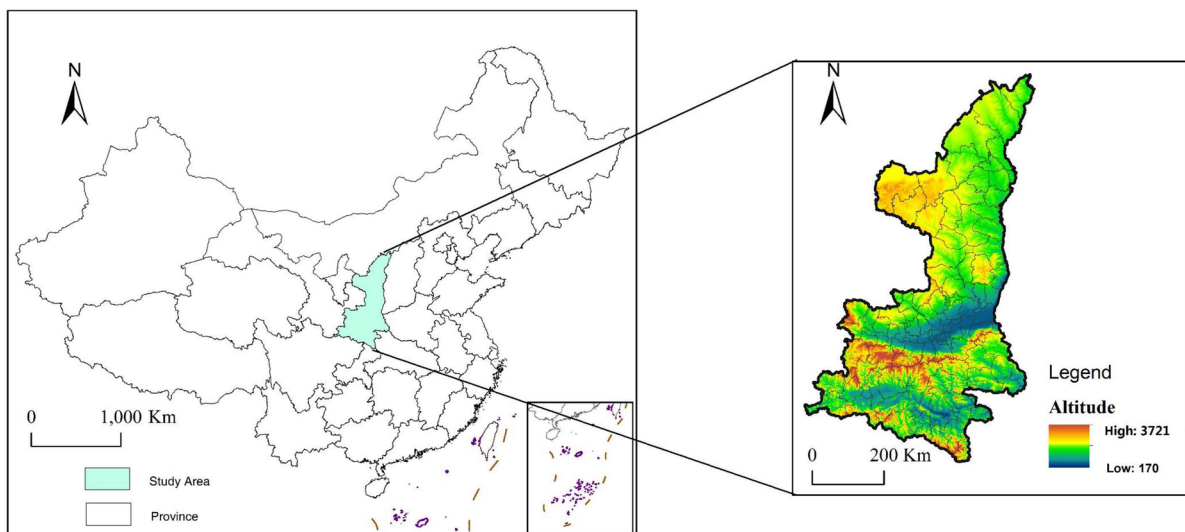


**Fig. 1** Location and elevation conditions of the counties in Shaanxi province
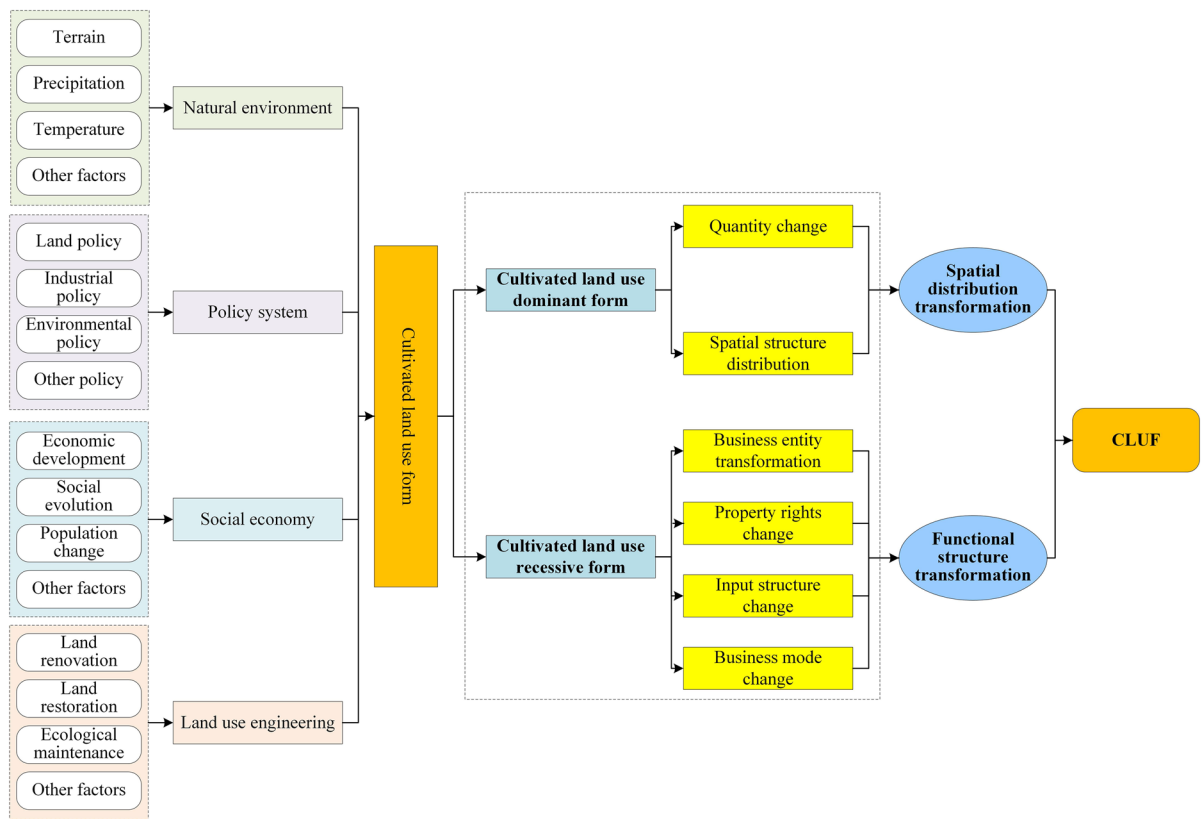
**Fig. 2** Conceptual framework of Cultivated Land Use Form

basic function of cultivated land is to ensure an adequate supply of food production. Therefore, the change in grain sown area per capita has an essential impact on the quantity pattern of cultivated land use. Secondly, the structure and spatial pattern of cultivated land use were investigated based on landscape patterns. The spatial distribution structure of cultivated land use was measured through the

landscape area of cultivated land patches (PLAND), and the degree of cultivated land use concentration was measured with the application of the farmland patch agglomeration index (FPAI). For the CLRF, it is difficult to measure and quantify the property rights, operating subjects, and operating modes of cultivated land through data due to the limitations of data and research availability and utilization. Finally,

**Table 1** Measurement index system of Cultivated Land Use Form

| Target layer | Rule layer | Index layer | Index abbreviation | Unit | Weight |
|---|---|---|---|---|---|
| CLUF | CLDF | Per-capita cultivated land area | PCLA | hm²/person | 0.4021 |
| | | Per-capita grain sown area | PGSA | hm²/person | 0.2032 |
| | | Landscape area of cultivated land patches | PLAND | % | 0.2373 |
| | | Farmland patch agglomeration index | FPAI | % | 0.1574 |
| | CLRF | Per unit area yield of grain | PUAY | kg/hm² | 0.0688 |
| | | Machinery input per unit cultivated area | MIPU | kWh/hm² | 0.2410 |
| | | Per-capita agricultural output value | PAOV | Yuan/person | 0.1849 |
| | | Number of people per unit cultivated land | NPPU | person/hm² | 0.5053 |

**Table 2** Changes of standard deviation ellipse parameters of CLUF

| Year | Barycentric coordinates | | Gravity shift | | | $\delta_x$ | $\delta_y$ | Azimuth angle |
|---|---|---|---|---|---|---|---|---|
| | Longitude | Latitude | Direction | Distance | Rate | | | |
| 2000 | 108°50′04″ | 34°53′29″ | – | – | – | 140.142 | 294.467 | 19.49 |
| 2005 | 108°50′29″ | 34°53′62″ | Northeast | 957 | 191 | 140.724 | 299.289 | 18.83 |
| 2010 | 108°50′17″ | 34°53′45″ | Southwest | 363 | 72.6 | 139.880 | 295.606 | 19.23 |
| 2015 | 108°49′51″ | 34°52′54″ | Southwest | 1972 | 394.4 | 140.631 | 294.565 | 19.48 |

four indexes of per unit area yield of grain (PUAY), machinery input per unit cultivated land (MIPU), the per-capita agricultural output value (PVOV), and the number of people per unit cultivated land (NPPU) were selected as proxy indexes for the measurement of recessive morphology of cultivated land use. Among them, the PUAY reflects the quality level of cultivated land utilization. The higher the PUAY, the better the quality of cultivated land; the MIPU mainly reflects the input intensity of cultivated land utilization; the PVOV mainly reflects the output function of cultivated land use; the NPPU mainly reflects the function of cultivated land use.

The CLUF was measured with the applications of the entropy weight method and linear combination method in the analyses above. The entropy method is the main method to calculate the weight of each indicator of the comprehensive evaluation index system, which can effectively avoid the subjective bias caused by artificially assigned indicator weights and eliminates information overlap and overlap between composite indicators (Zhao et al., 2018). The linear combination method mainly uses the calculated weight and index value of the entropy method to synthesize a single index. The organic combination of the two methods has become the most common method to obtain the corresponding evaluation index (Yang et al., 2018). The specific calculation steps are as follows:

Firstly, the range method is adopted to standardize each indicator to eliminate the difference in indicator dimensions. Since the measurement indicators of CLUF are positive, the formula is presented as below:

$$y_{ij} = \left[ x_{ij} - \min\left( x_{ij} \right) \right] / \left[ \max\left( x_{ij} \right) - \min(x_{ij}) \right] \tag{1}$$

where, $i$ represents each county; $j$ represents measurement indicators of CLUF; max and min represent the maximum and minimum values of the measurement indicators, respectively; $y_{ij}$ is the original value after standardization.

Secondly, all indicators are quantified with the same measurement to calculate the proportion of each county's $j$ th indicator $P_{ij}$ in each year. The formula is as follows:

$$P_{ij} = y_{ij} / \sum_{i=1}^{m} y_{ij} \tag{2}$$

Thirdly, the weight of each index in the measurement index system of CLUF is calculated; the formula is as follows:

$$W_j = \left[ 1 - \left( \sum_{i=1}^{m} P_{ij} \ln P_{ij} \right) / \ln m \right] / \sum_{i=1}^{n} \left[ 1 - \left( \sum_{i=1}^{m} P_{ij} \ln P_{ij} \right) / \ln m \right] \tag{3}$$

Fourthly, the value of CLUF is calculated with the weight measured by formula Eq. (3). The formula is shown as below:

$$CLUF_j = w_1 * CLDF + w_2 * CLRF \tag{4}$$

where, $w_1$ and $w_2$ are the weights of CLDF and CLRF, respectively.

Exploratory spatial data analysis methods

Exploratory spatial data analysis (ESDA), an essential technology of spatial statistical analysis, is mainly used to explain spatial dependence, spatial correlation, and spatial autocorrelation phenomena related to spatial location and to explore the general rules of the spatial distribution of objects through the description and visualization of spatial distribution pattern (Dou et al., 2016). Spatial autocorrelation includes both global and local autocorrelation. Global autocorrelation is used to test the general trend of spatial correlation of attribute values of adjacent or similar regional units throughout the study area, which is mainly measured by Global Moran's index with a value range from −1 to 1. Global Moran's index is less than 0, indicating a negative spatial correlation in the regional CLUF; Global Moran's index is greater

than 0, showing a positive spatial correlation in the regional CLUF; and the global Moran's index is equal to 0, indicating no spatial correlation in the regional CLUF. The formula is as follows:

$$Global\ Moran's\ I = \sum_{i=1}^{n} \sum_{j=1}^{n} W_{ij} \left(Y_i - \overline{Y}\right)\left(Y_j - \overline{Y}\right) / S^2 \sum_{i=1}^{n} \sum_{j=1}^{n} W_{ij} \quad (5)$$

where $S^2$ is the variance of CLUF; $Y_i$ and $Y_j$ are the observed values of CLUF in each county; $\overline{Y}$ is the average value of CLUF; $n$ is the observed number ($n = 107$); $W_{ij}$ is the spatial weight matrix. If there is a common boundary between region $i$ and region $j$, then $W_{ij} = 1$; if not, then $W_{ij} = 0$.

Global Moran's index can examine the spatial agglomeration status of CLUF throughout the region but cannot reflect the degree of correlation between CLUF and adjacent regions in a single region (Hu et al., 2019). In contrast, local Moran's index can express the degree of obedience of each local unit to the general global trend and the spatial heterogeneity (Hughey et al., 2018). The LISA cluster map is adopted to reflect the local spatial autocorrelation status, which is obtained through local Moran's index. The formula is displayed as below:

$$Local\ Moran's\ I = n\left(X_i - \overline{X}\right) \sum_{j=1}^{n} W_{ij}\left(X_j - \overline{X}\right) / \sum_{i=1}^{n} \left(X_i - \overline{X}\right)^2 \quad (6)$$

where $X_i$ and $X_j$ are the observed values of the CLUF in each county; $\overline{X}$ is the average value of the CLUF; $n$ is the observed number ($n = 107$); $W_{ij}$ is the spatial adjacency weight matrix. The local Moran's index greater than 0 indicates that the high (low) value of a certain area is surrounded by the high (low) value of the adjacent area, a typical "High-High" agglomeration or "Low-Low" agglomeration; the local Moran's index less than 0 demonstrates that the high (low) value of a certain area is surrounded by the low (high) value of the adjacent area, a typical "High-Low" agglomeration or "Low–High" agglomeration.

Standard deviational (SDE) analysis

Standard deviational ellipse (SDE) analysis, a spatial pattern statistical analysis method, is mainly used to reveal the spatial distribution characteristics and trends of research objects with wide application in geography, economics, and environmental analysis (Richter et al., 2021). SDE analysis mainly focuses on the analyses and calculation of the distribution center of gravity, the azimuth angle, the standard deviation of the semi-major axis, the semi-minor axis, and other attribute parameters to identify and judge the evolution process of geographic elements in the spatial distribution (Yang et al., 2020). Therefore, the SDE method was adopted here to identify the spatial distribution and evolution direction of the CLUF in Shaanxi province and to determine the spatial position change and movement trend of the center of gravity of the CLUF. The formula is as follows:

$$x' = x_i - x_{ave}\ ;\ y' = y_i - y_{ave} \quad (7)$$

where $x_{ave}$ and $y_{ave}$ are the average centers of $x_i$ and $y_i$; $x'$ and $y'$ are the relative coordinates of each point from the center of the area.

$$\tan\theta = \frac{\left(\sum_{i=1}^{n} W_i^2 x_i'^2 - \sum_{i=1}^{n} W_i^2 y_i'^2\right) + \sqrt{\left(\sum_{i=1}^{n} W_i^2 x_i' y_i' - \sum_{i=1}^{n} W_i^2 y_i'^2\right) + 4\left(\sum_{i=1}^{n} W_i^2 x_i' y_i'\right)}}{2\sum_{i=1}^{n} W_i^2 x_i^2 y_i^2} \quad (8)$$

where $W_i$ is the regional CLUF, and $\tan\theta$ is the corner of the distribution pattern of gravity center.

$$\delta_x = \sqrt{\sum_{i=1}^{n} \left(W_i x_i' \cos\theta - W_i y_i' \sin\theta\right)^2 / \sum_{i=1}^{n} W_i^2}$$

$$\delta_y = \sqrt{\sum_{i=1}^{n} \left(W_i x_i' \sin\theta - W_i y_i' \cos\theta\right)^2 / \sum_{i=1}^{n} W_i^2} \quad (9)$$

where $\delta_x$ and $\delta_y$ are respectively the standard deviations along the $X$-axis and $Y$-axis.

Kernel density estimation

Kernel density estimation is an analytical method to analyze the spatial distribution characteristics of

research objects' evaluation value, directly reflecting the degree of spatial dispersion and agglomeration of research objects (Wang et al., 2020a, b, c). Kernel density estimation uses a continuous density curve to describe the distribution position, shape, and extensibility of the research objects, which can reflect the CLUF level, regional difference, polarization degree, and the difference between the research object with the highest CLUF and other objects. Among them, the height and width of the wave crest reflect the difference between the objects, and the number of wave crest indicates the degree of polarization. The longer the tailing of distribution ductility, the more significant the difference between objects (Y. Hu et al., 2018). The kernel density estimation formula is as follows:

$$f(x) = \frac{1}{Nh} \sum_{i=1}^{N} K(\frac{X_i - \overline{x}}{h}) \tag{10}$$

where $N$ is the number of observations ($N = 107$); $X_i$ represents independent and identically distributed observations; $\overline{x}$ is the mean value of observations; $h$ is the bandwidth. Generally, the kernel density estimation is more sensitive to bandwidth, and the smaller the bandwidth, the higher the accuracy of the kernel density estimation results; and $K(\cdot)$ is the kernel density function, which usually satisfies:

$$\begin{cases} \lim_{x \to \infty} K(x) \bullet x = 0 \\ K(x) \geq 0, \int_{-\infty}^{+\infty} K(\chi)dx = 1 \\ \sup K(x) \prec +\infty, \int_{-\infty}^{+\infty} K^2(x)dx \prec +\infty \end{cases} \tag{11}$$

The kernel density estimates can be divided into triangular kernel density, quadrangular kernel density, and Gaussian kernel density. Here, Gaussian kernel density function is adopted to analyze the dynamic evolution of CLUF.

Multiple linear regression and spatial regression analysis

The formation mechanism of cultivated land use transition is relatively complicated, so are the factors that affect CLUF (Liang & Li, 2020). The multiple linear regression model is widely used to investigate the quantitative relationship between two or more variables, and it is also a standard model for studying driving factors. The formula is as follows:

$$Y_i = \beta_0 + \sum_{j=1}^{k} \beta_j X_{ij} + \varepsilon_i \tag{12}$$

where $Y_i$ is the dependent variable; $X_{ij}$ is the independent variable; $k$ is the number of observations; $\beta$ is the parameter to be estimated; $\varepsilon_i$ is the random error term.

The analytical from the OLS model framework has long been the primary method to investigate the multi-factor model. However, the existence of spatial dependence assumption was ignored, resulting in the bias of estimation results and inaccurate estimation values (Arnold & Wied, 2010). Spatial econometrics is a vital tool to solve the quantitative problem of spatial correlation. Anselin and Elhorst introduced spatial correlation into the traditional data model and gradually improved the spatial econometric model. Since then, the spatial autoregressive (SLM) model and spatial error (SEM) model have gained increasing application in spatial econometric models. The SLM model mainly examines the spatial influence and spillover effects of surrounding spatial units on the target unit. The specific formula is as follows:

$$Y = \rho WY + \beta X + \varepsilon \tag{13}$$

where $Y$ is the dependent variable matrix; $X$ is the $n$th order exogenous independent variable; $W$ is the $n$th order spatial adjacency matrix; $\varepsilon$ is the random error term; $\rho$ is the spatial regression coefficient, reflecting the degree of interpretation of the dependent variable by the adjacent spatial unit.

When the error term is spatially related, the SEM model can measure the spatial dependence effect existing in the error term and the impact of the error impact of the dependent variable in the neighboring area on the observed value of the region. The specific formula is as follows:

$$Y = \beta X + \mu \ , \ \mu = \lambda W \mu + \varepsilon \tag{14}$$

where $\mu$ is the random error term vector; $\lambda$ is the spatial correlation strength coefficient between the spatial regression residuals; $W$ is the $nth$ spatial adjacency matrix.

Data source

The data used in this study contain the data for constructing the CLUF Index system and data for the driving factors of the CLUF Index. For building CLUF Index system data, mainly use, the land use data were

collected from Resources and Environmental Science Data Center of China Academy of Sciences resources (http://www.resdc.cn/) in 2000, 2005, 2010, and 2015, to provide high spatial resolution remote sensing monitoring data, production data in each phase of the Landsat TM/ETM remote sensing image as the primary data source, generated by artificial visual interpretation. The land use types include cultivated land, woodland, grassland, water area, residential land, and unused land and 25 secondary land types. County land area, population, the acreage sown to grain, grain yield, and agricultural output data were mainly obtained from the Shaanxi provincial statistical yearbook, county statistical yearbook of China, and prefecture-level statistical yearbook and bulletin of Shaanxi province. For PLAND and FPAI data, that contains in cultivated land to use ArcGis10.2 software type combined with Fragstats software based on direct measurement. DEM data was provided by Geospatial Data Cloud Site, Chinese Academy of Sciences (http://www.gscloud.cn). DEM data is mainly based on the ASTER GDEM2 data with a spatial resolution of 30 m. This data is produced based on the detailed observations of NASA's new generation of earth observation satellite Terra. The annual mean precipitation data and annual mean temperature data were obtained from the annual mean temperature spatial interpolation data set and annual mean precipitation spatial interpolation data set of Resources and Environmental Science Data Center of Chinese Academy of Sciences (http://www.resdc.cn/). The data of GDP at the county level, per capita income of farmers, the output value of secondary and tertiary industries, investment in fixed assets, and urban population were mainly obtained from the Statistical Yearbook of Shaanxi province, Statistical Yearbook of China, Statistical Yearbook and Bulletin of Counties of Shaanxi province, and Government Work Report of Counties of Shaanxi province. Besides, administrative zoning data are available from the National Basic Geographic Information System (http://www.ngcc.cn/). The linear interpolation method was used to interpolate the missing values for some years.

## Results

### Analysis of spatial pattern evolution of CLUF

The CLUF, CLDF, and CLRF of 108 county-level administrative units in Shaanxi province from 2000 to 2015 were calculated with formula (4), and the cultivated land use the shape index for classification was analyzed with 5-level natural breakpoint method via the software ArcGIS 10.2.

Firstly, from the spatial distribution of CLUF (Fig. 3), it can be seen that the CLUF of the county showed apparent spatial differentiation in the study period, high in the middle, and low in the north and south, which was consistent with the terrain of Shaanxi province. In the central area of Shaanxi province sits the Guan Zhong plain with flat terrain fertile soil, abundant heat, and sufficient rainfall, where sufficient water irrigation can be achieved, making it the primary grain production area of Shaanxi province. In the southern part of Shaanxi province lies the Qinling Mountain. The terrain is mainly hilly and mountainous. This area with considerable annual average precipitation and high sensitivity of soil erosion is prone to mountain torrents, landslides, debris flows, and other natural disasters. The soil here is relatively poor, resulting in poor quality and low utilization of cultivated land. The northern part of Shaanxi province is a typical loess plateau. Due to the severe soil erosion caused by hills and gullies, the irrational use of land, and the continuous deterioration of the natural environment, the potential productivity of cultivated land resources failed to be unleashed, and the value of CLUF is low (Liu et al., 2020a, b). Secondly, from the perspective of CLUF value, the average value increased from 0.3019 in 2003 to 0.3646 in 2015, showing that the CLUF of the county is on the rise as a whole, and so is the degree of rationalization of cultivated land use. Thirdly, from the aspect of absolute value difference of CLUF, the highest value of CLUF in 2000 was 0.4937, the lowest value was 0.1066, and the absolute difference value was 0.3871. In 2015, the highest value of CLUF was 0.7291, the lowest value was 0.1074, and the absolute difference value was 0.6217. The expansion of the absolute difference value indicated that the overall difference of CLUF value within the county is gradually expanding.

The spatial distribution of CLDF is displayed in Fig. 4. Firstly, the spatial distribution of the CLDF is similar to that of the CLUF, showing a typical overall distribution pattern of high in the middle and low in the north and south. Secondly, the average values of CLDF in 2000, 2005, 2010, and 2015 were 0.2683, 0.2541, 0.2615, and 0.2503, respectively, indicating a decreasing trend of the CLDF in all counties from 2000 to 2015.
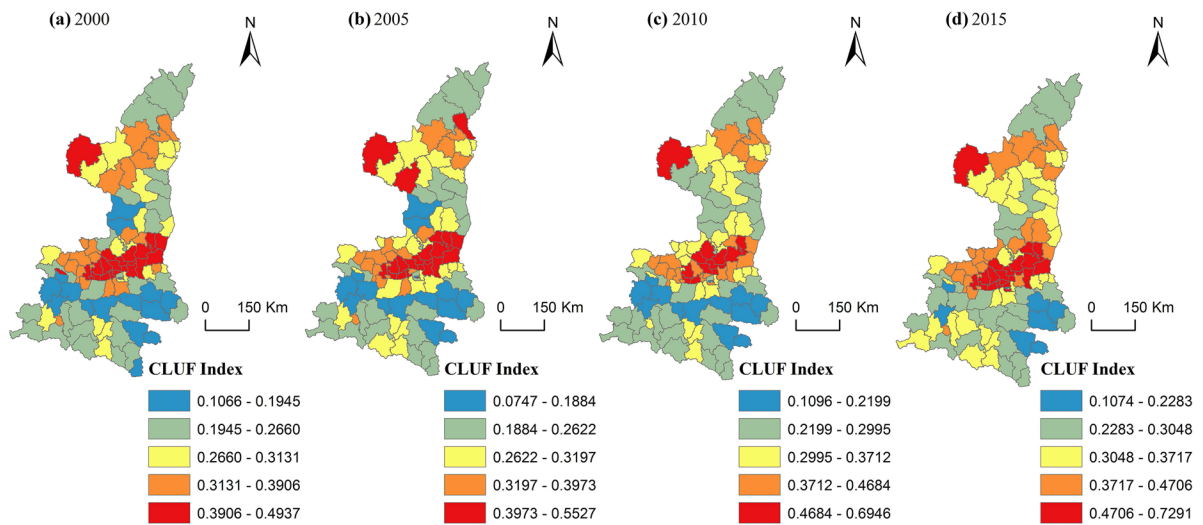
**Fig. 3** Spatial distribution of Cultivated Land Use Form

The spatial distribution of the CLRF is shown in Fig. 5. Firstly, the spatial distribution of CLRF is similar to those of CLUF and the CLDF, a typical distribution of high in the middle and low in the north and south. Secondly, the average value of the CLRF in Shaanxi province in 2000 was 0.0335, while the average value of each county in 2015 was 0.1144, higher than that of CLRF in 2000. The average number of counties was 30, and it rose to 36 in 2015. Thirdly, in terms of local distribution perspective, the CLRF in some counties in the northern and central areas of Shaanxi province increased year by year from

2000 to 2015, while the CLRF in southern regions showed no significant change, even showing a trend of deterioration.

Spatial correlation analysis of CLUF

To shed light on the spatial correlation of CLUF, the global Moran's index of CLUF was calculated by GeoDa software based on spatial adjacency weight matrix, and the Z-value test was carried out. As shown in Fig. 6, the global Moran's index for CLUF
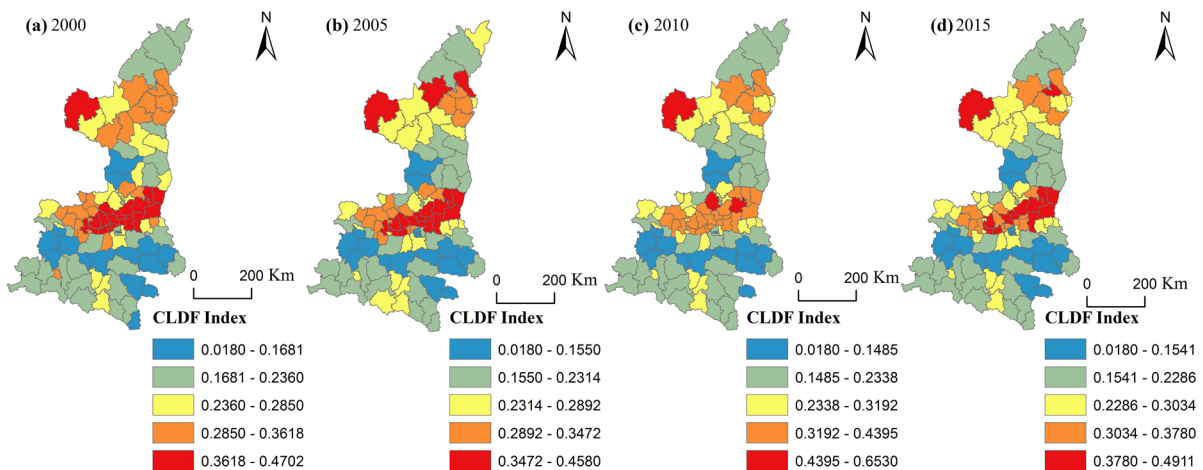


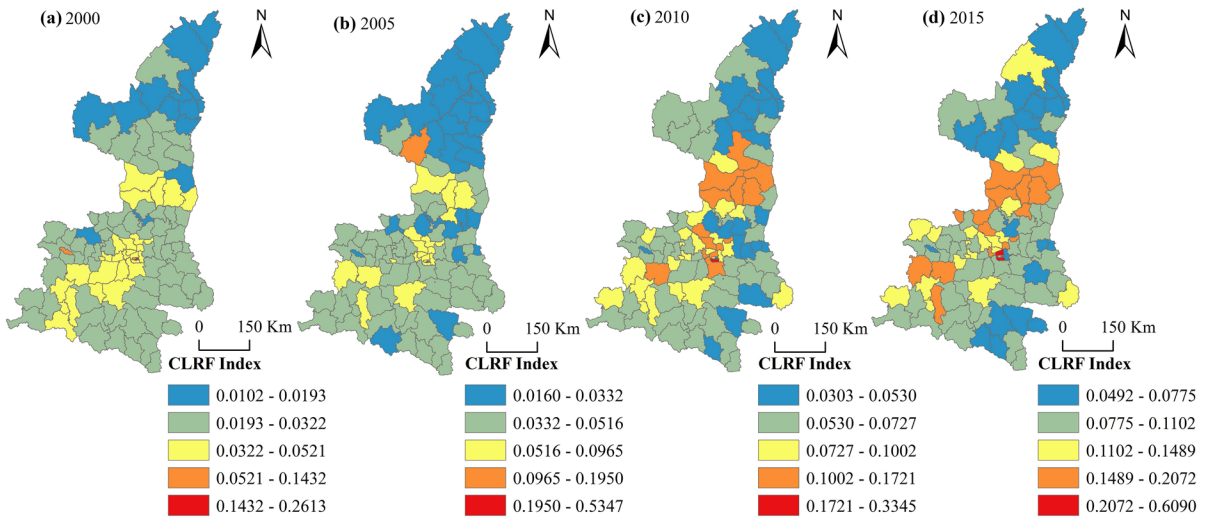**Fig. 4** The spatial distribution of the cultivated land use dominant form index

**Fig. 5** The spatial distribution of the cultivated land use recessive form index

was positive for each county from 2000 to 2015, which are 0.554, 0.446, 0.536, and 0.455, respectively, and all pass the 1% significance level test, indicating that the CLUF of counties has an obvious global spatial positive correlation, and the CLUF of a county is affected by the CLUF of adjacent regions. In addition, the spatial agglomeration of CLUF is similar among regions.
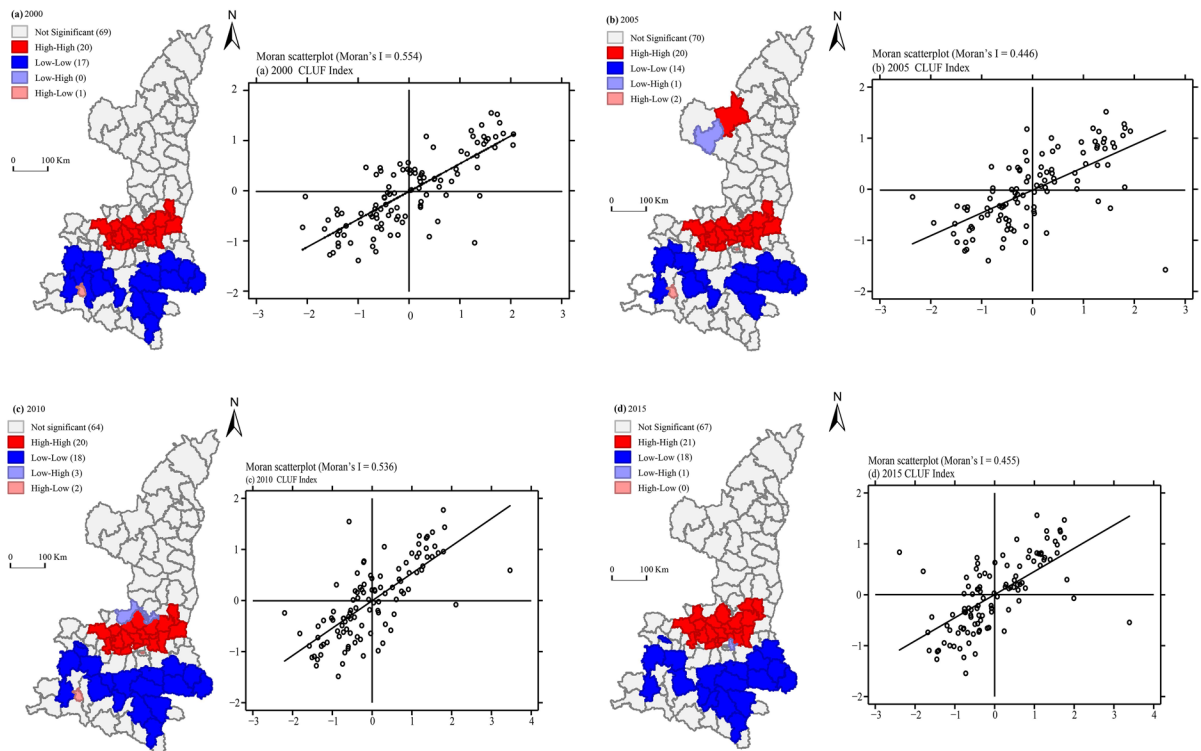


**Fig. 6** The spatial correlation of the Cultivated Land Use Form index

Given the limitations of Global Moran's index in showing the spatial agglomeration characteristics of a specific area, the existence of local agglomeration phenomenon in CLUF was explored by the combination of Moran scatter diagram and local Moran index, and the selected LISA cluster diagram (Fig. 6) of CLUF in 2000, 2005, 2010, and 2015. The local spatial distribution of CLUF can be divided into four types: The first type is the "High-High" agglomeration type, which means that the CLUF of the county and the neighboring counties are high. The overall performance is a high-level spatially balanced and associated agglomeration state of "high center and high surroundings." The number of counties with high agglomeration was stable at 20 from 2000 to 2010 and increased to 21 in 2015. The second type is the "Low–High" agglomeration type, which means that the CLUF of the county is low, but the CLUF of its neighboring counties is high. The overall performance is a spatial imbalance of "low center and high surroundings"–associated agglomeration. The number of counties with low and high agglomeration increased from 0 to 3 in 2000 to 2010 and then decreased to 1 in 2015. The third type is "Low-Low" agglomeration, which means that the CLUF of the county and the neighboring counties are low. The overall performance is a low-level spatial equilibrium agglomeration state of "low center and low surroundings." The number of low agglomeration counties decreased from 17 to 14 from 2000 to 2005 and then increased to 18 in 2010 and 2015. The fourth type is the "High-Low" agglomeration, which means that the CLUF of the county is high, but the CLUF in the neighboring counties is low. The overall performance is a spatial non-equilibrium agglomeration state of "high center surroundings." The number of high-low agglomeration counties increased from 1 to 2 from 2000 to 2010 and then decreased to 0 in 2015.

In general, the local spatial pattern of CLUF in Shaanxi province during the study period showed apparent coexistence of high-high and low-low agglomeration, which indicated that the CLUF of counties had a noticeable spatial proximity peer effect. When the CLUF of neighboring counties presented a high level, the county was more likely to be the county administrative unit with high level CLUF, and vice versa. This effect is consistent with the Matthew effect. At the same time, from the perspective of the overall agglomeration trend, the CLUF

of counties presented the centralized distribution of high-high and low-low agglomeration, discrete distribution of low–high agglomeration, and high-low agglomeration, which indicates that the CLUF of counties showed spatial proximity spillover effect in geographical location.

Standard deviational ellipse analysis of CLUF

To accurately reveal the spatial evolution trend of the CLUF, the elliptical distribution and the center of gravity shift trend of the CLUF in 2000, 2005, 2010, and 2015 (Fig. 7) were plotted using the SDE spatial statistical analysis tool of ArcGIS 10.2 software. The center of gravity of the CLUF moved between $108°49' - 108°50'E$ and $34°52' - 34°53'N$ from 2000 to 2015. The center of gravity of the CLUF moved to the northeast from 2000 to 2005 and moved back to the southwest from 2005 to 2015. However, during the study period, the center of gravity of the CLUF was all located in the central part of Shaanxi province, indicating that the CLUF at the county level was relatively stable in spatial distribution during the study period, and the overall spatial distribution of the central part was strong in the north and south parts.

According to Table 2, the gravity center of CLUF had a small range of movement from a minimum movement of 363 m to a maximum movement of 1972 m from 2000 to 2015. The gravity center's maximum moving rate is 394.4 m/year, and the minimum is 72.6 m/year. The moving rate first decreases and then increases, indicating that the variation degree of CLUF first decreases and then increases. In terms of the change in azimuth angle, the angle first decreased from 19.49° in 2000 to 18.83° in 2005 and then continued to increase to 19.48° in 2015. In the X-axis direction, the standard deviation increased from 140.142 km in 2000 to 140.724 km in 2005, then decreased to 139.880 km in 2010, and finally increased to 140.631 km in 2015, indicating that the CLUF presents a trend of "dispersion-agglomeration-redispersion" in the X-axis direction. In the Y-axis direction, the standard deviation increased from 294.467 km in 2000 to 299.289 km and then decreased to 294.565 km in 2015, indicating that the CLUF showed a "dispersion-agglomeration" fluctuation trend in the Y-axis direction. According to the standard deviation data of the X-axis and Y-axis, the
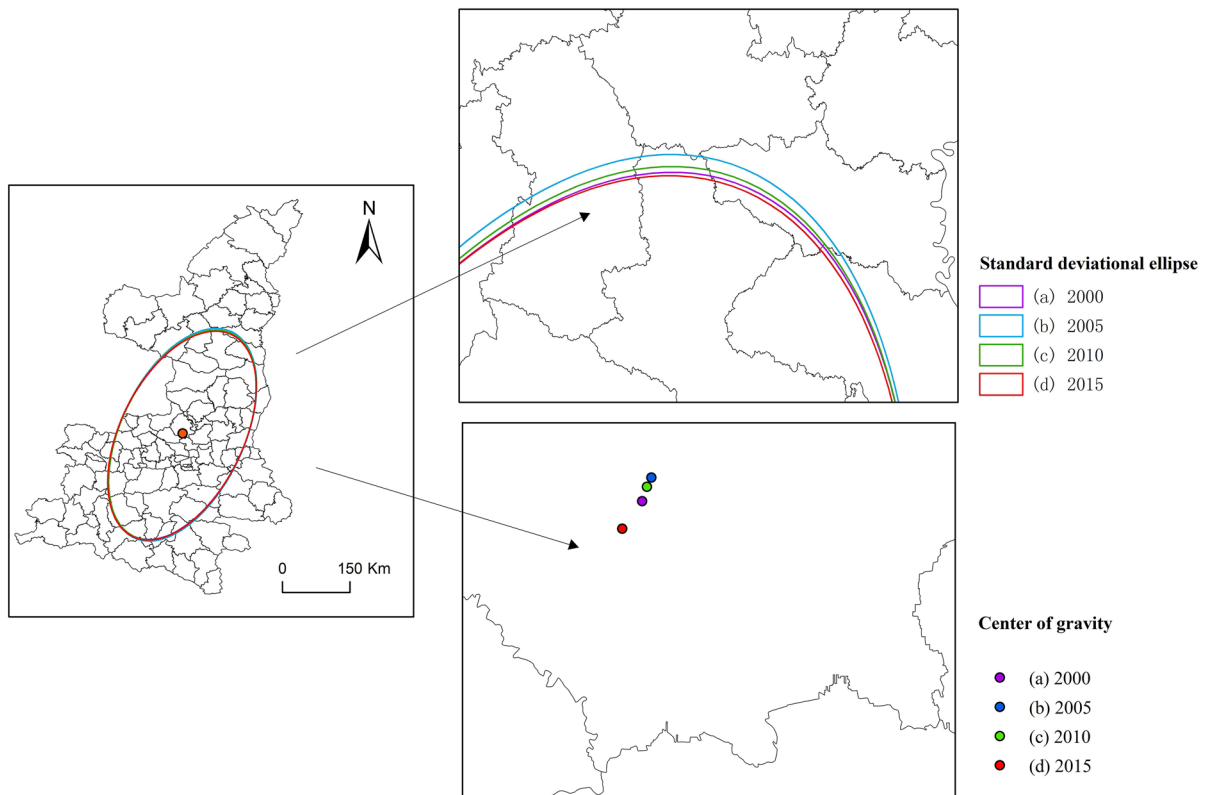
**Fig. 7** Standard deviational ellipse analysis of CLUF

standard deviation of CLUF along the *X*-axis and *Y*-axis increased and then decreased, indicating that CLUF along *X*-axis and *Y*-axis distributed from divergence to concentration.

Kernel density estimation of CLUF

The results were calculated using the kernel density estimation formula eq. (11). The kernel density curves of CLUF in 2000, 2005, 2010, and 2015 (Fig. 8) were drawn by STATA16.0. Furthermore, the dynamic evolution of the time series of CLUF was characterized.

From the curve of kernel density of CLUF, it can be found that (1) in terms of the gravity center position of the curve, the gravity center position of the curve moved to the left from 2000 to 2005 and then to the right from 2005 to 2015, indicating that the value of CLUF showed a decline first and then a rise in the study period. (2) The peak height of the

curve's central peak showed the peaks rose slightly from 2000 to 2005 and then slumped from 2005 to 2010, suggesting that the difference in the cultivated CLUF between counties showed a trend of first shrinking and then expanding. In 2005, returning farmland to the forest in northern Shaanxi had been implemented for about five years. The continuous return of farmland to forestry and grassland in the region had a sharp decline in the absolute amount of cultivated land. Currently, counties in the central region have been vigorously implemented water-saving transformation in irrigation districts and agricultural mechanization projects (Dang et al., 2020). The two differentiated policies have caused a rapidly increasing variation in cultivated land use patterns among counties in the province. (3) In terms of the number of curve peaks, the coexistence of the central peak and a secondary peak in 2000–2015 revealed a polarization pattern of CLUF in the county during the study period. (4) In terms of the left and right tailing of the curve, the right tailing of
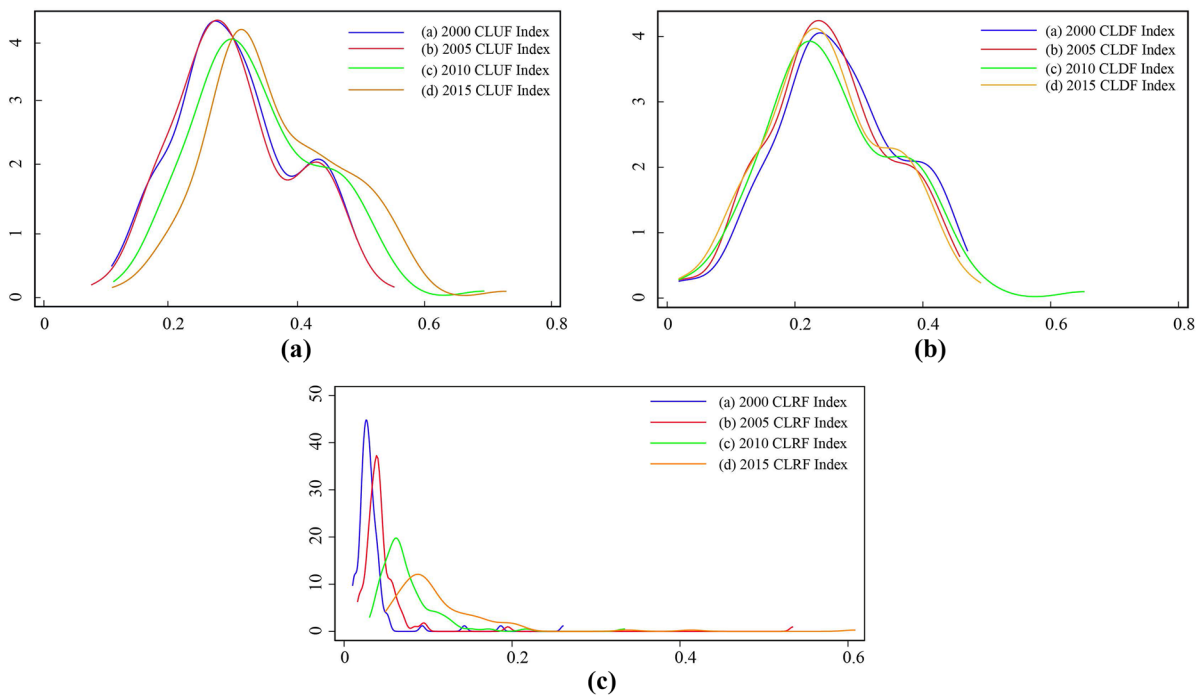
**Fig. 8** kernel density estimation of CLUF

the curve was larger than the left tailing from 2000 to 2015. In addition, there was a trend of elongation and thickening of the tails, indicating that the CLUF pattern in high-value counties had increased during the study period and that the number of high-value counties increased.

From the curve of kernel density of CLDF, it can be found that (1) in terms of the position of the gravity center, the gravity center of the curve shifted to the left during 2000–2010, and then shifted to the right during 2010–2015, indicating that the CLDF decreased first and then increased during the study period. (2) From the perspective of the height of the central peak of the curve, the peak of the central peak of the curve showed a "rising-declining-rising" trend from 2000 to 2015, indicating that the difference of the CLDF among counties showed a trend of "reducing- increasing- reducing." (3) From the number of curve peaks, the central peak and the secondary peak coexisted in 2000–2015 suggested that the CLDF in the study period had a polarization pattern. (4) From the left and right tail of the curve, the right side of the curve shortened from 2000 to 2005,

increased from 2005 to 2010, and decreased again from 2010 to 2015.

From the curve of kernel density of CLRF, it can be found that (1) in terms of the gravity center position, the gravity center of the curve from 2000 to 2015 moved to the right, indicating an over-all upward trend of CLRF in the study period. (2) From the peak height of the curve's main peak, the central peak continued to decline from 2000 to 2015, indicating an overall narrowing of the gap of the CLRF among counties in the study period. (3) In terms of the number of curve peaks, the central peak, and multiple secondary peaks coexisted from 2000 to 2015, and the central peak and secondary peaks coexisted from 2010 to 2015, indicating that the distribution pattern of CLRF in the study period first existed polarization, and gradually turned to multipolar distribution pattern. (4) From the left and right tail of the curve, the curve's right tail continued to grow from 2000 to 2015, illustrating the continued growth of CLRF in high-value area counties and the increase in the proportion of counties in the high-value area.

Analysis of the driving mechanism of CLUF pattern differentiation

*The conceptual framework of the driving mechanism of CLUF*

The land use transition results from the interaction and mutual restriction of multiple factors such as natural environmental conditions, socio-economic systems, land governance engineering technology, government laws and regulations, and regional population conditions in a specific area (Tian et al., 2020). The CLUF is essential for land use transition. As the most basic agricultural production condition, cultivated land carries an adequate supply of food and the source of essential food for human survival. The transformation of cultivated land use is affected by the specific social, economic, political, and cultural factors in the region and the regional natural environment, traffic location, and population changes (Su et al., 2019). The driving factors of CLUF are multi-level, including the natural environment, economic growth, government policies, and urbanization development. The natural environment, economic growth, and urbanization development were selected as drivers influencing CLUF due to the challenging nature of measuring government policy factors in the

jurisdiction and the fact that socio-economic factors and urbanization development factors are the driving outcomes of government policies (Fig. 9).

According to the above theoretical analysis framework, nine indicators of three categories were selected as the essential of cultivated land use transition (Table 3). The natural environment factors, including elevation (DEM), annual mean temperature (MAT), and annual mean precipitation (MAP), are essential factors affecting the distribution and utilization efficiency of cultivated land. Since the differences in topography and hydrological factors will lead to uneven distribution of cultivated land resources and determine regional agricultural production mode, the natural environment factors are also critical to determine the direction of use and realize the benefit of harvest in the use of cultivated land. The elements of economic growth include per capita GDP(GPC), farmers' capita net income (FCN), and the ratio of secondary and tertiary industries (RST). The cultivated land transition is usually associated with regional social and economic development. On the one hand, social and economic growth can weaken the agricultural production value of cultivated land, and the property income value brought by cultivated land transformation becomes more prominent. On the other



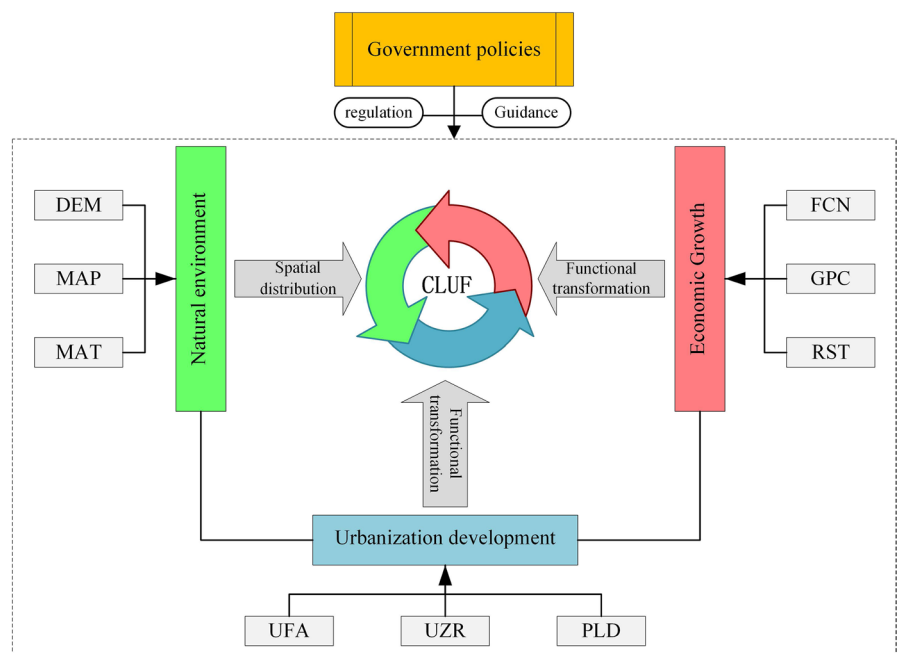**Fig. 9** Conceptual frame diagram of the driving mechanism of CLUF

**Table 3** Driving factors of cultivated land use transition

| Rule layer | Index layer | Index abbreviation | Description |
|---|---|---|---|
| Natural environment | Elevation | *DEM* | County average elevation |
| | Annual mean precipitation | *MAP* | Regional precipitation conditions |
| | Annual mean temperature | *MAT* | Regional temperature conditions |
| Economic growth | Per capita GDP | *GPC* | Regional economic development level |
| | Farmers capital net income | *FCN* | Farmers income level |
| | Ratio of secondary and tertiary industries | *RST* | Industrial structure level |
| Urbanization development | Urban fixed asset investment per land | *UFA* | Regional investment level |
| | Urbanization rate | *UZR* | Regional urbanization level |
| | Population density | *PLD* | Population carrying capacity |

hand, with social and economic development, the potential demand for food supply will be greater, which will increase the burden of arable land use. Three indicators of urban fixed asset investment per land (UFA), urbanization rate (UZR), and population density (PLD) are chosen for urbanization development factors. While the urbanization development drives the gradual migration of rural labor to cities and towns, the non-agriculturalization of cultivated land, hollowing out of the rural population, and occupation of cultivated land for construction land disordering and other phenomena will also emerge. Simultaneously, the abandonment and over-utilization of cultivated land alongside the abandonment of homesteads will impact the cultivated land transition.

*Result analysis of driving factors*

Spatial econometric regression for the driving mechanism of cultivated land use transition from 2000 to 2015 requires LM test and a robust LM test to determine whether a spatial lag model or a spatial error model is chosen (Baltagi & Bresson, 2011). According to the results in Table 4, Moran's index in 2010 and 2015 did not pass the 10% robustness test in SEM test, while the LM test in 2010 and the robust LM test in 2010 and 2015 both passed the 10% robustness test. In SLM test, it was found that the LM test of spatial lag and spatial error and the robust LM test of other years mostly passed the significance test, except for the robust LM test of 2015. Therefore, the SLM model was selected for spatial econometric regression.

According to OLS and SLM model regression results at the county level (Table 5), the cultivated land use transition at the county level results from the natural environment, economic growth, and urbanization development. (1) DEM had a positive correlation with the CLUF at the significance level of 10% in 2000 and 2010, and a negative correlation with the CLUF at the significance level of 5% in 2015, which

**Table 4** Model selection test of spatial effect

| Test | 2000 | | 2005 | | 2010 | | 2015 | |
|---|---|---|---|---|---|---|---|---|
| | Statistic | *P*-value | Statistic | *P*-value | Statistic | *P*-value | Statistic | *P*-value |
| SEM test | | | | | | | | |
| Moran's index | 1.529 | 0.126 | 1.706 | 0.088 | 1.355 | 0.175 | 1.058 | 0.290 |
| Lagrange Multiplier | 17.169 | 0.000 | 21.461 | 0.000 | 7.163 | 0.007 | 1.356 | 0.244 |
| Robust Lagrange Multiplier | 8.835 | 0.003 | 14.052 | 0.000 | 2.331 | 0.127 | 0.281 | 0.596 |
| SLM test | | | | | | | | |
| Lagrange Multiplier | 15.568 | 0.000 | 9.060 | 0.003 | 11.029 | 0.001 | 3.472 | 0.062 |
| Robust Lagrange Multiplier | 7.233 | 0.007 | 1.650 | 0.199 | 6.197 | 0.013 | 2.397 | 0.122 |

**Table 5** Spatial regression analysis results of driving factors of cultivated land use transition

| | 2000 | | 2005 | | 2010 | | 2015 | |
|---|---|---|---|---|---|---|---|---|
| | OLS | SLM | OLS | SLM | OLS | SLM | OLS | SLM |
| DEM | 0.063 | 0.113[a] | 0.027 | 0.074 | 0.052 | 0.125[a] | − 0.230[c] | − 0.172[b] |
| | (0.062) | (0.065) | (0.065) | (0.050) | (0.081) | (0.076) | (0.071) | (0.073) |
| MAP | − 0.240[c] | − 0.241[c] | − 0.205[c] | − 0.200[c] | − 0.261[c] | − 0.267[c] | − 0.070 | − 0.088[a] |
| | (0.040) | (0.044) | (0.038) | (0.032) | (0.055) | (0.050) | (0.049) | (0.047) |
| MAT | 0.579[c] | 0.658[c] | 0.393[b] | 0.468[c] | 0.473[b] | 0.641[c] | − 0.195 | − 0.065 |
| | (0.156) | (0.164) | (0.158) | (0.110) | (0.215) | (0.200) | (0.187) | (0.187) |
| GPC | 0.028[b] | 0.022[b] | 0.031[a] | 0.031[b] | 0.014 | 0.025 | 0.058[b] | 0.063[c] |
| | (0.014) | (0.011) | (0.018) | (0.012) | (0.022) | (0.020) | (0.023) | (0.022) |
| FCN | − 0.001 | − 0.014 | − 0.001 | − 0.009 | − 0.010 | − 0.009 | − 0.062 | − 0.071 |
| | (0.020) | (0.022) | (0.026) | (0.028) | (0.053) | (0.048) | (0.049) | (0.046) |
| RST | − 0.116[b] | − 0.085[b] | − 0.212[c] | − 0.179[c] | − 0.183[c] | − 0.138[b] | − 0.309[c] | − 0.281[c] |
| | (0.046) | (0.037) | (0.050) | (0.043) | (0.059) | (0.055) | (0.065) | (0.063) |
| UFA | − 0.002 | − 0.003 | − 0.005 | − 0.006 | 0.016 | 0.007 | 0.024[c] | 0.021[c] |
| | (0.006) | (0.006) | (0.007) | (0.007) | (0.010) | (0.009) | (0.008) | (0.008) |
| UZR | − 0.034 | − 0.021 | 0.030 | 0.013 | 0.043 | 0.009 | 0.002 | − 0.017 |
| | (0.039) | (0.030) | (0.061) | (0.046) | (0.052) | (0.048) | (0.049) | (0.047) |
| PLD | − 0.039[a] | − 0.020 | 0.012 | 0.028 | − 0.102[c] | − 0.065[b] | − 0.126[c] | − 0.109[c] |
| | (0.020) | (0.019) | (0.020) | (0.047) | (0.029) | (0.028) | (0.027) | (0.027) |
| Cons | − 0.915 | − 1.558[a] | − 0.098 | − 0.814 | − 0.018 | − 1.391 | 3.526[c] | 2.666[b] |
| | (0.907) | (0.924) | (1.005) | (0.785) | (1.371) | (1.300) | (1.308) | (1.301) |
| W-Y | – | 0.038[c] | – | 0.035[c] | – | 0.038[c] | – | 0.022[a] |
| | | (0.009) | | (0.010) | | (0.011) | | (0.011) |
| $R^2$ | 0.603 | 0.656 | 0.479 | 0.522 | 0.513 | 0.561 | 0.549 | 0.565 |
| LogL | – | 159.404 | – | 138.702 | – | 135.756 | – | 131.783 |
| AIC | − 283.594 | − 294.808 | − 248.210 | − 253.404 | − 240.188 | − 247.512 | − 239.850 | − 239.565 |
| BIC | − 256.865 | − 262.734 | − 221.482 | − 221.330 | − 213.460 | − 215.438 | − 213.122 | − 207.492 |

[a, b, c] represents significant correlation at the significance level of 10%, 5%, and 1%, respectively.

Standard errors are in parentheses

significantly impacted the spatial pattern of cultivated land use. The northern counties of Shaanxi province are located in the Loess Plateau area at a high altitude. From 2000 to 2010, due to the comprehensive treatment and ecological restoration work, most of the abandoned land became high-standard construction farmland through slope farmland management and warping dam construction. Therefore, the utilization of cultivated land showed a transition trend of increasing quantity and improving quality. During 2015, with the in-depth development of the farmland management project and rapid socio-economic development, the altitude has seriously restricted the rational development of cultivated land resources by the main body of cultivated land utilization, resulting in the reduction of the number of cultivated land utilization and the contraction of local space. (2) MAP showed a significantly negative correlation with the CLUF, but the negative correlation was gradually less marked. This probably Shaanxi province is located in the northwest inland region, and the average annual precipitation decreases from the southeast to the northwest inland. Due to the low precipitation, the water resources for agricultural production are incredibly scarce, resulting in a transformation pattern of the reduced amount of cultivated land and spatial shrinkage. MAT is the opposite. MAT from 2000 to 2010 showed a significant positive correlation with the CLUF. The high average annual temperature provides light and heat conditions for agricultural

production, which in turn accelerated the melting process of glaciers in rivers. Large amounts of glacier meltwater can alleviate water shortage and ensure the amount of water required for agricultural production. Utilization shows a relative increase in quantity. At the same time, the transition of cultivated land use to quantity and quality improvement has been facilitated. (3) Except in 2010, GPC has a significant positive impact on the CLUF, and the degree of impact has deepened over time. The industrial-technological progress induced by economic development can promote the transformation of agricultural production methods and the innovation of production technology. The output benefit of cultivated land continues to increase, which in turn induces the cultivated land use transition to the direction of relative quality improvement (Huaranca et al., 2019). (4) RST has a significant negative impact on the CLUF during the study period. The increase in RST has led to a decline in the proportion of agricultural production in the total output value of Shaanxi province. In addition, the rapid growth of the secondary and tertiary industries will occupy a large number of arable land resources, resulting in a reduction in cultivated land utilization and a shrinking spatial transition. (5) PLD has a significant negative impact on the CLUF. The increase of PLD will increase the land carrying capacity and the pressure on the ecological environment. The supporting service facilities and population living space will also reduce the cultivated land area (Wellmann et al., 2020), leading to the reduction type transition of cultivated land quantity.

## Discussion

Based on the data of 107 counties in Shaanxi province in 2000, 2005, 2010, and 2015, the CLUF was measured using the entropy weight method and linear sum method. The dynamic evolution rules and spatial differentiation characteristics of cultivated land use transition in the county were described from a two-dimensional spatiotemporal perspective. At the same time, the driving mechanism affecting the differentiation of cultivated land use transition patterns was also empirically analyzed, and the following research conclusions and implications were obtained.

This study mainly uses spatial statistical analysis tools to analyze the land use transition in Shaanxi

province. The study found that the overall cultivated land use situation in Shaanxi province was gradually rationalized. In terms of specific spatial forms, the county-level cultivated land use form index showed a spatial differentiation pattern of high in the middle and low in the north and south. Shaanxi province has a continental monsoon climate, and the north and south climate zones are temperate, warm temperate, and subtropical. The temperature and precipitation in Shaanxi province gradually increased from north to south, and the main vegetation types in the region have prominent zonal characteristics, including temperate grassland, forest-steppe interlaced zone, and broad-leaved forest (Wang et al., 2020a, b, c). The central part of Shaanxi province is mainly the Guanzhong Plain of Shaanxi province, the main grain-producing area in the region, where rainfall, light, and heat are sufficient (Wu et al., 2022), so the degree of intensive use of cultivated land here is relatively high. Yang and Huang (2019) also confirmed this view, as the northern region of Shaanxi province is an energy and chemical industry base, with the development of resources not only puts pressure on the ecological environment but also causes air pollution and sewage pollution, which reduces the quality of environmental management. The implementation of air pollution control and a series of ecological projects in the central Guanzhong Plain in Shaanxi province will lead to a better greening of the region, which will promote the efficient use of resources in the region.

In addition, it was found that there was a strong positive spatial correlation between the cultivated land use pattern indices in Shaanxi province, and the local spatial differentiation pattern was dominated by high-high and low-low clustering. There was a trend of expanding decentralization to contracting concentration in geographic space, and the rationalization of cultivated land use among counties was improved. Practically speaking, natural geographical conditions have a significant impact on the pattern of cultivated land use, and although northern Shaanxi has arid and water-scarce climatic conditions, hilly and ravine landscapes, and plateau topography that can limit the development of agriculture and the effective use of cultivated land (Sun, 2018; Wei et al., 2018). In recent years, the government has improved irrigation technology by building reservoirs, dams, water cellars, and other water conservation facilities and the government has significantly improved the utilization

of arable land in northern Shaanxi by building reservoirs, dams, water cellars, and other water conservation facilities, improving irrigation technology, and increasing water utilization in recent years (Gao & Huang, 2020; Wen & Théau, 2020). In contrast, in the southern and central regions of Shaanxi province, the rational adjustment of land, arable land protection measures, and the improvement of agricultural production conditions and management levels have been achieved (Kang et al., 2018). The above measures have led to a gradual increase in the intensity of arable land use in Shaanxi province (Tang et al., 2015; Yang & Zhang, 2021).

The study also explored the factors influencing the transformation of cultivated land use, and we found that the transformation of cultivated land use is the result of a combination of the natural environment, economic growth, and urbanization factors in the county and that population density has a significant adverse effect on the transformation of cultivated land use. This view has been confirmed by scholars who have analyzed the change in arable land use and its main determinants in Tanzania, and the results of the study pointed out that demographic and socioeconomic factors have been identified to have a more significant impact on the change in the amount of arable land in Tanzania (Uisso & Tanrıvermiş, 2021). In addition, some scholars have pointed out that rapid economic development has contributed to an increase in the intensity of capital and technological inputs, and non-agricultural employment opportunities in cities have attracted much of the rural labor force (Su et al., 2019), leading to a decrease in the intensity of labor inputs and a decrease in rural population density, and the extent of farmers' use of arable land can be significantly weakened (Liang et al., 2021).

In this study, CLUF was constructed from a two-dimensional perspective of dominant and recessive forms to explore the cultivated land use transition in Shaanxi province. However, there are still some limitations in the research. First, due to data collection limitations, the evaluation index system of CLUF in this study cannot cover all the dominant and recessive forms of cultivated land use. Besides, because this research is based on one province of Shaanxi, this research results may differ from those of other provinces. In the following research, this research method will be applied to study other provinces in China to explore the differences in spatial analysis

characteristics and driving mechanisms of cultivated land use transition in different regions.

## Conclusions and policy recommendations

### Conclusions

The transformation of cultivated land use is of great significance in promoting the transformational development of the countryside and the improvement of its socio-economic level. In this study, the spatial statistical analysis tools and spatial regression analysis methods were used to analyze the spatial differentiation characteristics of arable land use transformation and its influencing factors in counties of Shaanxi province under the condition of measuring the cultivated land use morphological index, which measured the transformation status of cultivated land use from both explicit and implicit morphological aspects. Based on the analysis and findings, the following conclusions were drawn.

(a) In terms of spatial pattern evolution trend, the CLUF presents the spatial differentiation pattern of high in the central part and low in the north and south part, correlated with the Shaanxi province's terrain distribution pattern. (b) In terms of spatial autocorrelation analysis, there is a solid spatial positive correlation between CLUF. The local spatial differentiation pattern is mainly high-high agglomeration and low-low agglomeration. The high-high agglomeration areas are primarily located in the central regions of Shaanxi province, and the low-low agglomeration areas, in the southern regions. (c) In terms of ellipse standard deviation analysis, the center of gravity of CLUF moved from northeast to southwest in the study period; the CLUF shows a trend of expansion decentralization to contraction centralization in the physical space, with a noticeable spatial spillover effect. (d) In terms of kernel density estimation, the difference of CLUF during the study period shows a trend of first narrowing and then expanding; the difference of CLDF, first narrowing and then expanding and then narrowing; and the difference of CLRF, continuous narrowing. (e) The cultivated land use transition results from the interaction of natural environment, economic growth, and urbanization development factors in the county. The impact direction of DEM on CLUF changed from positive to negative;

MAP, RST, and PLD continued to be negative; MAT continued to be positive.

Policy recommendations

(1) The cultivated land use transition provides essential support for realizing China's agricultural modernization. Following the general law of economic development, it is necessary to increase the investment in regional science and technology levels, promote the application of advanced agricultural production technology and production tools, and promote cultivated land's rational use. Simultaneously, the construction of agricultural infrastructure and high-standard farmland construction projects should be strengthened to improve the efficiency and functional benefits of cultivated land use, and to guide the rational transformation and the development of cultivated land use.

(2) The differences in geographical location, resource endowments, and economic development of different counties should be fully considered. Moreover, the promotion of inter-regional cultivated land use calls for diversified cultivated land use security systems and mechanisms for counties and the implementation of county-based and localized policies. The balanced evolution of cultivated land is expected to improve cultivated land quality and output efficiency from institutional guarantees, improve the spatial form of cultivated land use, and promote the rational transformation and development of cultivated land use.

(3) The spatial spillover effect of cultivated land use change at the county level, as well as the demonstration role of counties with high CLUF index, needs to be used wisely to promote advanced, cultivated land management concepts and effective management practices to surrounding counties. At the same time, counties with a low CLUF index should both avoid the trend of unwinding and learn the experience and practices of other regions to stimulate the motivation of self-innovation, to improve the efficiency of cultivated land use, perfect the function of cultivated land, and to realize the standardized transformation and development of cultivated land use.

## Declarations

**Ethics approval**  Not applicable.

**Consent to participate**  Not applicable.

**Consent for publication**  Not applicable.

**Competing interests**  The authors declare no competing interests.

## References

Arnold, M., & Wied, D. (2010). Improved GMM estimation of the spatial autoregressive error model. *Economics Letters, 108*(1), 65–68. https://doi.org/10.1016/j.econlet.2010.04.012

Baltagi, B. H., & Bresson, G. (2011). Maximum likelihood estimation and Lagrange multiplier tests for panel seemingly unrelated regressions with spatial lag and spatial errors: An application to hedonic housing prices in Paris. *Journal of Urban Economics, 69*(1), 24–42. https://doi.org/10.1016/j.jue.2010.08.007

Deal, B., & Schunk, D. (2004). Spatial dynamic modeling and urban land use transformation: A simulation approach to assessing the costs of urban sprawl - ScienceDirect. *Ecological Economics, 51*(1–2),79–95.

Chen, R., Ye, C., Cai, Y., Xing, X., & Chen, Q. (2014). The impact of rural out-migration on land use transition in China: Past, present and trend. *Land Use Policy, 40*, 101–110. https://doi.org/10.1016/j.landusepol.2013.10.003

Dang, X., Gao, S., Tao, R., Liu, G., Xia, Z., Fan, L., & Bi, W. (2020). Do environmental conservation programs contribute to sustainable livelihoods? Evidence from China's grain-for-green program in northern Shaanxi province. *Science of the Total Environment, 719*, 137436. https://doi.org/10.1016/j.scitotenv.2020.137436

Deng, S. (2020). Exploring the relationship between new-type urbanization and sustainable urban land use:

Evidence from prefecture-level cities in China. *Sustainable Computing: Informatics and Systems*. https://doi.org/10.1016/j.suscom.2020.100446

Dou, Y., Luo, X., Dong, L., Wu, C., Liang, H., & Ren, J. (2016). An empirical study on transit-oriented low-carbon urban land use planning: Exploratory Spatial Data Analysis (ESDA) on Shanghai, China. *Habitat International, 53*, 379–389. https://doi.org/10.1016/j.habitatint.2015.12.005

Duro, J. A., Lauk, C., Kastner, T., Erb, K.-H., & Haberl, H. (2020). Global inequalities in food consumption, cropland demand and land-use efficiency: A decomposition analysis. *Global Environmental Change, 64*, 102124. https://doi.org/10.1016/j.gloenvcha.2020.102124

Gao, H., & Huang, Y. (2020). Impacts of the Three-North shelter forest program on the main soil nutrients in Northern Shaanxi China: A meta-analysis. *Forest Ecology and Management, 458*, 117808. https://doi.org/10.1016/j.foreco.2019.117808

Ge, D., Long, H., Zhang, Y., Ma, L., & Li, T. (2018). Farmland transition and its influences on grain production in China. *Land Use Policy, 70*, 94–105. https://doi.org/10.1016/j.landusepol.2017.10.010

Hu, M., Li, Z., Wang, Y., Jiao, M., Li, M., & Xia, B. (2019). Spatio-temporal changes in ecosystem service value in response to land-use/cover changes in the Pearl River Delta. *Resources, Conservation and Recycling, 149*, 106–114. https://doi.org/10.1016/j.resconrec.2019.05.032

Hu, Y., Wang, F., Guin, C., & Zhu, H. (2018). A spatio-temporal kernel density estimation framework for predictive crime hotspot mapping and evaluation. *Applied Geography, 99*, 89–97. https://doi.org/10.1016/j.apgeog.2018.08.001

Huaranca, L. L., Iribarnegaray, M. A., Albesa, F., Volante, J. N., Brannstrom, C., & Seghezzo, L. (2019). Social perspectives on deforestation, land use change, and economic development in an expanding agricultural frontier in Northern Argentina. *Ecological Economics, 165*, 106424. https://doi.org/10.1016/j.ecolecon.2019.106424

Hughey, S. M., Kaczynski, A. T., Porter, D. E., Hibbert, J., Turner-McGrievy, G., & Liu, J. (2018). Spatial clustering patterns of child weight status in a southeastern US county. *Applied Geography, 99*, 12–21. https://doi.org/10.1016/j.apgeog.2018.07.016

Kang, H., Tao, W., Chang, Y., Zhang, Y., Xuxiang, L., & Chen, P. (2018). A feasible method for the division of ecological vulnerability and its driving forces in Southern Shaanxi. *Journal of Cleaner Production, 205*, 619–628. https://doi.org/10.1016/j.jclepro.2018.09.109

Liang, X., Jin, X., Sun, R., Han, B., Liu, J., & Zhou, Y. (2021). A typical phenomenon of cultivated land use in China's economically developed areas: Anti-intensification in Jiangsu Province. *Land Use Policy, 102*, 105223. https://doi.org/10.1016/j.landusepol.2020.105223

Liang, X., & Li, Y. (2020). Identification of spatial coupling between cultivated land functional transformation and settlements in Three Gorges Reservoir Area. *China. Habitat International, 104*, 102236. https://doi.org/10.1016/j.habitatint.2020.102236

Liu, D., Chen, H., Geng, T., Zhang, H., & Shi, Q. (2020a). Spatiotemporal changes of regional ecological risks in Shaanxi Province based on geomorphologic regionalization Developing a novel proximity analysis approach for assessment of waste management cost efficiency in low population density regions. *Progress in Geography, 39*(2), 243–254. https://doi.org/10.18306/dlkxjz.2020a.02.006

Liu, J., Jin, X., Xu, W., Gu, Z., Yang, X., Ren, J., et al. (2020b). A new framework of land use efficiency for the coordination among food, economy and ecology in regional development. *Science of the Total Environment, 710*, 135670. https://doi.org/10.1016/j.scitotenv.2019.135670

Long, H., Ge, D., & Wang, J. (2019). Progress and prospects of the coupling research on land use transitions and rural transformation development. *Acta Geographica Sinica, 74*(12), 2546–2559.

Long, H., & Qu, Y. (2018). Land use transitions and land management: A mutual feedback perspective. *Land Use Policy, 74*, 111–120. https://doi.org/10.1016/j.landusepol.2017.03.021

Ma, L., Long, H., Tu, S., Zhang, Y., & Zheng, Y. (2020). Farmland transition in China and its policy implications. *Land Use Policy, 92*, 104470. https://doi.org/10.1016/j.landusepol.2020.104470

Mather, A. S., & Needle, C. L. (1998). The forest transition: A theoretical basis. *Area, 30*(2),117–124.

Perring, M. P., Standish, R. J., & Hobbs, R. J. (2013). Incorporating novelty and novel ecosystems into restoration planning and practice in the 21st century. *Ecological Processes, 2*(1), 18. https://doi.org/10.1186/2192-1709-2-18

Richter, A., Ng, K. T. W., Karimi, N., & Chang, W. (2021). Developing a novel proximity analysis approach for assessment of waste management cost efficiency in low population density regions. *Sustainable Cities and Society, 65*, 102583. https://doi.org/10.1016/j.scs.2020.102583

Song, X., & Li, X. (2019). Theoretical explanation and case study of regional cultivated land use function transition. *Acta Geographica Sinica, 74*(5), 992–1010. https://doi.org/10.11821/dlxb201905012

Su, M., Guo, R., & Hong, W. (2019). Institutional transition and implementation path for cultivated land protection in highly urbanized regions: A case study of Shenzhen, China. *Land Use Policy, 81*, 493–501. https://doi.org/10.1016/j.landusepol.2018.11.015

Sun, Y. (2018). The coupling relationship between the transformation of cultivated land utilization and grain yield in Shaanxi. *Chinese Journal of Agricultural Resources and Regional Planning, 39*(7), 14–20.

Tang, J., Folmer, H., & Xue, J. (2015). Technical and allocative efficiency of irrigation water use in the Guanzhong Plain, China. *Food Policy, 50*, 43–52. https://doi.org/10.1016/j.foodpol.2014.10.008

Tang, M., Li, Z., Hu, F., & Wu, B. (2020). How does land urbanization promote urban eco-efficiency? The mediating effect of industrial structure advancement. *Journal of Cleaner Production, 272*, 122798. https://doi.org/10.1016/j.jclepro.2020.122798

Tian, J., Wang, B., Zhang, C., Li, W., & Wang, S. (2020). Mechanism of regional land use transition in underdeveloped areas of China: A case study of northeast China. *Land Use Policy, 94*, 104538. https://doi.org/10.1016/j.landusepol.2020.104538

Uisso, A. M., & Tanrıvermiş, H. (2021). Driving factors and assessment of changes in the use of arable land in Tanzania. *Land Use Policy, 104*, 105359. https://doi.org/10.1016/j.landusepol.2021.105359

Wang, H., Liu, G., Li, Z., Zhang, L., & Wang, Z. (2020a). Processes and driving forces for changing vegetation ecosystem services: Insights from the Shaanxi Province of China. *Ecological Indicators, 112*, 106105. https://doi.org/10.1016/j.ecolind.2020.106105

Wang, H., & Zhang, G. (2021). Temporal variation in soil erodibility indices for five typical land use types on the Loess Plateau of China. *Geoderma, 381*, 114695. https://doi.org/10.1016/j.geoderma.2020.114695

Wang, S., Liu, H., Pu, H., & Yang, H. (2020b). Spatial disparity and hierarchical cluster analysis of final energy consumption in China. *Energy, 197*, 117195. https://doi.org/10.1016/j.energy.2020.117195

Wang, Z., Xu, X., Wang, H., & Meng, S. (2020c). Does land reserve system improve quality of urbanization? *Evidence from China. Habitat International, 106*, 102291. https://doi.org/10.1016/j.habitatint.2020.102291

Wei, X., Wang, S., Yuan, X., Wang, X., & Zhang, B. (2018). (240AD). Spatial and temporal changes and its variation of cultivated land quality in Shaanxi Province. *Transactions of the Chinese Society of Agricultural Engineering (Transactions of the CSAE), 34*(3).

Wellmann, T., Schug, F., Haase, D., Pflugmacher, D., & van der Linden, S. (2020). Green growth? On the relation between population density, land use and vegetation cover fractions in a city using a 30-years Landsat time series. *Landscape and Urban Planning, 202*, 103857. https://doi.org/10.1016/j.landurbplan.2020.103857

Wen, X., & Théau, J. (2020). Spatiotemporal analysis of water-related ecosystem services under ecological restoration scenarios: A case study in northern Shaanxi. *China. Science of the Total Environment, 720*, 137477. https://doi.org/10.1016/j.scitotenv.2020.137477

Wu, jiujiang, Wang, N., Shen, H., & Ma, X. (2022). Spatial–temporal variation of climate and its impact on winter wheat production in Guanzhong Plain. *China. Computers and Electronics in Agriculture, 195*, 106820. https://doi.org/10.1016/j.compag.2022.106820

Xiang, J., Li, J., & Zeng, J. (2016). Spatial difference and its influence factors of cultivated land transition of poverty counties in west of Hubei. *Transactions of the Chinese Society of Agricultural Engineering, 32*(1), 272–279. https://doi.org/10.11975/j.issn.1002-6819.2016.01.038

Yang, D., Luan, W., Qiao, L., & Pratama, M. (2020). Modeling and spatio-temporal analysis of city-level carbon emissions based on nighttime light satellite imagery. *Applied Energy, 268*, 114696. https://doi.org/10.1016/j.apenergy.2020.114696

Yang, Q., & Zhang, D. (2021). The influence of agricultural industrial policy on non-grain production of cultivated land: A case study of the "one village, one product" strategy implemented in Guanzhong Plain of China. *Land Use Policy, 108*, 105579. https://doi.org/10.1016/j.landusepol.2021.105579

Yang, W., Xu, K., Lian, J., Ma, C., & Bin, L. (2018). Integrated flood vulnerability assessment approach based on TOPSIS and Shannon entropy methods. *Ecological Indicators, 89*, 269–280. https://doi.org/10.1016/j.ecolind.2018.02.015

Yang, Y., & Huang, P. (2019). Has the level of green development in the northwestern provinces of China truly improved? A case study of Shaanxi. *Sustainable Cities and Society, 51*, 101779. https://doi.org/10.1016/j.scs.2019.101779

Zeilhofer, P., Cezar, A., Tres, N. M., De, A. J., Anah T., & Silveira, L. (2014). Jaguar Panthera onca habitat modeling in landscapes facing high land-use transformation pressure – Findings from Mato Grosso Brazil. *Biotropica, 46*(1), 98–105.

Zhao, J., Ji, G., Tian, Y., Chen, Y., & Wang, Z. (2018). Environmental vulnerability assessment for mainland China based on entropy method. *Ecological Indicators, 91*, 410–422. https://doi.org/10.1016/j.ecolind.2018.04.016